

Spin-dependent terms of the Breit-Pauli Hamiltonian evaluated with explicitly correlated Gaussian basis set for molecular computations

Péter Jeszenszki,¹ Péter Hollósy,¹ Ádám Margócsy,¹ and Edit Mátyus^{1,*}

¹*MTA-ELTE ‘Momentum’ Molecular Quantum electro-Dynamics Research Group,
Institute of Chemistry, Eötvös Loránd University,
Pázmány Péter sétány 1/A, Budapest, H-1117, Hungary*

(Dated: 23 June 2025)

This work compiles the spin-dependent leading-order relativistic and quantum electrodynamical corrections to the electronic structure of atoms and molecules within the non-relativistic quantum electrodynamics framework. We report the computation of perturbative corrections using an explicitly correlated Gaussian basis set, which allows high-precision computations for few-electron systems. In addition to numerical tests for triplet Be, triplet H₂, and triplet H₃⁺ states and comparison with no-pair Dirac–Coulomb–Breit Hamiltonian energies, numerical results are reported for electronically excited states of the triplet helium dimer, He₂, for which the present implementation delivers high-precision magnetic coupling curves necessary for a quantitative understanding of the fine structure of its high-resolution rovibronic spectrum.

I. INTRODUCTION

Few-electron atoms and molecules are sometimes referred to as ‘calculable’ systems, which allow to extensively test and extend the frontier of current methodologies and probe small physical effects by comparison with high-resolution spectroscopy experiments. At the extreme of precision physics applications, the most accurate experimental and most possible complete theoretical treatments for ionization, dissociation and rovibrational energies progress head-to-head [1–3], and ultimately deliver more precise values for fundamental physical constants and set bounds on possible new types of forces [4, 5]. Furthermore, the reliable identification of quantum states is crucial for the manipulation of atoms and molecules with laser light, which contributes to advancements in the field of ultracold molecules [6] and quantum technologies [7, 8]. Theoretical and computational progress in precision physics delivers benchmark values for quantum chemistry methods targeting larger systems.

For few-particle systems, an explicitly correlated basis set is frequently applied in combination with a variational procedure to capture the essential electron-electron correlation effects, leading to fast convergence in energy and other physical properties [9, 10]. To obtain analytic expressions for the matrix elements, floating Explicitly Correlated Gaussians (fECGs) are used as a spatial basis set [9–13], for which numerical efficiency in the high-precision computation of few-electron systems has already been demonstrated [14–21].

Since the electronic energy of few-particle systems can be converged to high-precision in a variational fECG approach, the relativistic and quantum electrodynamical (QED) contributions become ‘visible’ and important even for (compounds of) light elements. High-resolution spectroscopic measurements reveal small magnetic effects, seen as fine and hyperfine splittings in the spectra. We will refer to the relevant interactions as ‘spin-dependent’ relativistic (and QED) interactions, and we will also use the term ‘spin-independent’ relativistic and QED corrections, which give contributions to the centroid energy. While the computation of the centroid corrections is well elaborated, including the regularization techniques [22–24], which enhance the convergence of singular terms in the Gaussian basis representation (for the missing incorrect electron-nucleus and electron-electron coalescence behaviour).

In this paper, we focus on the fECG-based implementation of the spin-dependent matrix elements of the Breit–Pauli Hamiltonian. We also include corrections for the anomalous magnetic moment of the electron, which constitute the leading-order ($\alpha^3 E_h$, with the α fine structure constant) QED corrections to the spin-dependent terms. We note that higher-order QED ($\alpha^4 E_h$) corrections have been derived by Douglas and Kroll in 1974 for the helium atom triplet states [25] and more recently, the $\alpha^5 E_h$ order corrections non-radiative, radiative and recoil corrections have been derived and evaluated for triplet helium states [18, 26]. Inner shell transitions are in excellent agreement with experiment, though there is a significant deviation for the ionization energy between theory [27, 28] and experiment [29–32].

The present work focuses on the relativistic leading-order QED corrections, *i.e.*, up to $\alpha^3 E_h$ order, but goes beyond atomic applications; molecular systems require the development of a floating ECG methodology, reported in the present work.

* edit.matyus@ttk.elte.hu

Non-floating, spherically symmetric, ECG basis sets have already been successfully used in spin-dependent atomic computations, considering beryllium, boron and carbon atomic states [19, 33–37].

In this paper, we report a general N -particle implementation without restrictions on the number and spatial arrangement of the atomic nuclei. The implementation is based on a spinor basis representation, in which the spatial and spin components are evaluated independently and subsequently combined via calculating simple tensor products. The approach is, in principle, ‘general’ and not restricted by the number of particles or point-group symmetry. For testing the developed methodology, we perform computations for triplet Be for comparison with literature values. Two-electron triplet H_2 and also two-electron triplet H_3^+ (both a linear and a triangular configuration) are compared with our in-house developed no-pair DCB computations [38].

Then, as a first application of the methodology, we compute magnetic coupling curves for several electronically excited states of the triplet He_2 molecule, which significantly improve upon previously available values using standard quantum chemistry methodologies [39–45]. These newly-computed coupling curves are used in rovibronic-fine-structure computations reported in separate papers [46, 47].

II. THEORETICAL FRAMEWORK

For atoms and molecules with low nuclear charge, the non-relativistic description often provides a good starting point. The non-relativistic electronic energy is incremented with relativistic and QED corrections arranged according to powers of the fine-structure constant, α . In this paper, we include all terms up to α^3 (in Hartree atomic units),

$$E = E^{(0)} + \alpha^2 E^{(2)} + \alpha^3 E^{(3)} . \quad (1)$$

We start by solving the Schrödinger equation,

$$\hat{H}^{(0)}|\varphi^{(0)}\rangle = E^{(0)}|\varphi^{(0)}\rangle , \quad (2)$$

where the non-relativistic electronic Hamiltonian is

$$\hat{H}^{(0)} = -\frac{\hbar^2}{2m} \sum_{i=1}^{n_{el}} \Delta_{\mathbf{r}_i} - \sum_{i=1}^{n_{el}} \sum_{A=1}^{N_{nuc}} \frac{Z_A}{r_{iA}} + \sum_{i=1}^{n_{el}} \sum_{j>i}^{n_{el}} \frac{1}{r_{ij}} , \quad (3)$$

with the nuclei clamped at \mathbf{R}_A . We use the short notation, $r_{iX} = |\mathbf{r}_{iX}|$, $\mathbf{r}_{iA} = \mathbf{r}_i - \mathbf{R}_A$, and $\mathbf{r}_{ij} = \mathbf{r}_i - \mathbf{r}_j$.

The leading-order relativistic corrections, $\alpha^2 E^{(2)}$, can be computed using the non-relativistic wave function, $\varphi^{(0)}$, as the expectation value of the Breit-Pauli (BP) Hamiltonian. The focus of this work is the computation of the spin-dependent contributions, so we write the Hamiltonian as the sum of spin-independent (sn) and spin-dependent (sd) terms [48, 49]

$$\hat{H}^{(2)} = \hat{H}_{sn}^{(2)} + \hat{H}_{sd}^{(2)} = \hat{H}_{MV} + \hat{H}_{D1} + \hat{H}_{OO} + \hat{H}_{D2} + \hat{H}_{SO} + \hat{H}_{SOO} + \hat{H}_{SOO'} + \hat{H}_{SOO} + \hat{H}_{SS} , \quad (4)$$

where the manifestly spin-independent terms are re-iterated only for completeness, *i.e.*, the mass-velocity (MV), the Darwin one (D1), the Darwin two (D2), and the orbit-orbit terms (OO) are

$$\hat{H}_{MV} = -\frac{1}{8} \sum_{i=1}^{n_{el}} (\hat{\mathbf{p}}_i^2)^2 , \quad \hat{H}_{D1} = \frac{\pi}{2} \sum_{i=1}^{n_{el}} \sum_{A=1}^{N_{nuc}} Z_A \delta(\mathbf{r}_{iA}) , \quad \hat{H}_{D2} = -\pi \sum_{i=1}^{n_{el}} \sum_{j>i}^{n_{el}} \delta(\mathbf{r}_{ij}) , \quad (5)$$

and

$$\hat{H}_{OO} = -\frac{1}{2} \sum_{i=1}^{n_{el}} \sum_{j>i}^{n_{el}} \left[\frac{1}{r_{ij}} \hat{\mathbf{p}}_i \hat{\mathbf{p}}_j + \frac{1}{r_{ij}^3} (\mathbf{r}_{ij} (\mathbf{r}_{ij} \hat{\mathbf{p}}_j) \hat{\mathbf{p}}_i) \right] . \quad (6)$$

The corrections carrying spin operators in their expressions are the spin-orbit interaction, with $\hat{\mathbf{l}}_{iX} = \mathbf{r}_{iX} \times \hat{\mathbf{p}}_i$ and $\hat{\mathbf{s}}_i = \frac{1}{2} I(1) \otimes \dots \otimes \boldsymbol{\sigma}(i) \otimes \dots \otimes I(n_{el})$ with the $\boldsymbol{\sigma} = (\sigma_x, \sigma_y, \sigma_z)$ Pauli matrices,

$$\hat{H}_{SO} = \frac{1}{2} \sum_{i=1}^{n_{el}} \sum_{A=1}^{N_{nuc}} \frac{Z_A}{r_{iA}^3} \hat{\mathbf{s}}_i \hat{\mathbf{l}}_{iA} , \quad (7)$$

the spin-own-orbit interaction,

$$\hat{H}_{\text{SOO}} = -\frac{1}{2} \sum_{i=1}^{n_{\text{el}}} \sum_{j>i}^{n_{\text{el}}} \frac{1}{r_{ij}^3} \left[\hat{\mathbf{s}}_i \hat{\mathbf{l}}_{ij} + \hat{\mathbf{s}}_j \hat{\mathbf{l}}_{ji} \right], \quad (8)$$

the spin-other-orbit interaction,

$$\hat{H}_{\text{SOO}'} = -\sum_{i=1}^{n_{\text{el}}} \sum_{j>i}^{n_{\text{el}}} \frac{1}{r_{ij}^3} \left[\hat{\mathbf{s}}_i \hat{\mathbf{l}}_{ji} + \hat{\mathbf{s}}_j \hat{\mathbf{l}}_{ij} \right], \quad (9)$$

and the spin-spin interaction,

$$\hat{H}_{\text{SS}} = \sum_{i=1}^{n_{\text{el}}} \sum_{j>i}^{n_{\text{el}}} \left[(\hat{\mathbf{s}}_i \hat{\mathbf{s}}_j) (\hat{\mathbf{p}}_i \hat{\mathbf{p}}_j \frac{1}{r_{ij}}) - (\hat{\mathbf{s}}_i \hat{\mathbf{p}}_j) (\hat{\mathbf{s}}_j \hat{\mathbf{p}}_i \frac{1}{r_{ij}}) \right] = \hat{H}_{\text{SS,dp}} + \hat{H}_{\text{SS,c}}, \quad (10)$$

which is written as the sum of the magnetic dipole-dipole interaction,

$$\hat{H}_{\text{SS,dp}} = \sum_{i=1}^{n_{\text{el}}} \sum_{j>i}^{n_{\text{el}}} \left[\frac{\hat{\mathbf{s}}_i \hat{\mathbf{s}}_j}{r_{ij}^3} - \frac{3(\hat{\mathbf{s}}_i \mathbf{r}_{ij})(\hat{\mathbf{s}}_j \mathbf{r}_{ij})}{r_{ij}^5} \right] \quad (11)$$

and the Fermi contact term,

$$\hat{H}_{\text{SS,c}} = -\frac{8\pi}{3} \sum_{i=1}^{n_{\text{el}}} \sum_{j>i}^{n_{\text{el}}} \hat{\mathbf{s}}_i \hat{\mathbf{s}}_j \delta(\mathbf{r}_{ij}) = -2\pi \sum_{i=1}^{n_{\text{el}}} \sum_{j>i}^{n_{\text{el}}} \delta(\mathbf{r}_{ij}), \quad (12)$$

where in the last step we used the form of the Fermi contact term over the anti-symmetrized Hilbert subspace.

The spin-independent terms, giving rise to the relativistic correction of the ‘centroid’ are collected as

$$\alpha^2 \hat{H}_{\text{sn}}^{(2)} = \alpha^2 [\hat{H}_{\text{MV}} + \hat{H}_{\text{D1}} + \hat{H}_{\text{OO}} + \hat{H}_{\text{D2}} + \hat{H}_{\text{SS,c}}]. \quad (13)$$

The precise computation of expectation values (with Gaussian basis sets) for this part has been discussed in detail elsewhere [22–24].

The focus of the present work is the implementation of the spin-dependent terms

$$\alpha^2 \hat{H}_{\text{sd}}^{(2)} = \alpha^2 \left[\hat{H}_{\text{SO}} + \hat{H}_{\text{SOO}} + \hat{H}_{\text{SOO}'} + \hat{H}_{\text{SS,dp}} \right]. \quad (14)$$

In addition, we consider the effect of the anomalous magnetic moment of the electron [50–52] on the spin-dependent terms, giving rise to the leading-order QED correction for the spin-dependent part,

$$\alpha^3 \hat{H}_{\text{sd}}^{(3)} = \alpha^2 \left[\frac{\alpha}{\pi} \hat{H}_{\text{SO}} + \frac{\alpha}{\pi} \hat{H}_{\text{SOO}} + \frac{1}{2} \frac{\alpha}{\pi} \hat{H}_{\text{SOO}'} + \frac{\alpha}{\pi} \hat{H}_{\text{SS,dp}} \right]. \quad (15)$$

So, up to $\alpha^3 E_{\text{h}}$ order, the spin-dependent terms are

$$\alpha^2 \hat{H}_{\text{sd}} = \alpha^2 \left[\left(1 + \frac{\alpha}{\pi}\right) \hat{H}_{\text{SO}} + \left(1 + \frac{\alpha}{\pi}\right) \hat{H}_{\text{SOO}} + \left(1 + \frac{\alpha}{2\pi}\right) \hat{H}_{\text{SOO}'} + \left(1 + \frac{\alpha}{\pi}\right) \hat{H}_{\text{SS,dp}} \right]. \quad (16)$$

III. IMPLEMENTATION

For the numerical implementation, the non-relativistic wave function is expanded in an explicitly correlated basis set,

$$|\varphi^{(\Gamma, SM_S)}\rangle = \sum_{\mu=1}^N C_{\mu} |\phi_{\mu}^{(\Gamma, SM_S)}\rangle, \quad (17)$$

where the coefficients C_μ are obtained by diagonalizing the non-relativistic Hamiltonian matrix. We define the basis function as

$$\phi_\mu^{(\Gamma, SM_S)} = \phi^{(\Gamma, SM_S)}(\mathbf{r}; \mathbf{A}_\mu, \mathbf{s}_\mu, \boldsymbol{\theta}_\mu) = \hat{\mathcal{A}}\{f^{(\Gamma)}(\mathbf{r}; \mathbf{A}_\mu, \mathbf{s}_\mu)\chi^{(SM_S)}(\boldsymbol{\theta}_\mu)\}. \quad (18)$$

$\chi^{(SM_S)}(\boldsymbol{\theta}_\mu)$ is a spin function, $f^{(\Gamma)}(\mathbf{r}; \mathbf{A}_\mu, \mathbf{s}_\mu)$ is a spatial function. In this work, it is the symmetrized floating explicitly correlated Gaussian function (fECG) [9–13]

$$f_\mu^{(\Gamma)} = f^{(\Gamma)}(\mathbf{r}; \mathbf{A}_\mu, \mathbf{s}_\mu) = \hat{\mathcal{P}}_\Gamma \exp[-(\mathbf{r} - \mathbf{s}_\mu)^T (\mathbf{A}_\mu \otimes \mathbf{I}_3)(\mathbf{r} - \mathbf{s}_\mu)] , \quad (19)$$

where $\hat{\mathcal{P}}_\Gamma$ is the projector onto the Γ irreducible representation (irrep) of the point-group defined by the fixed nuclear skeleton, \mathbf{I}_3 is the three-dimensional identity matrix, \mathbf{A}_μ and \mathbf{s}_μ are parameters to be optimized by minimization of the non-relativistic energy.

$\hat{\mathcal{A}}$ is the anti-symmetrization operator for the electrons,

$$\hat{\mathcal{A}} = (N_{\text{perm}})^{-\frac{1}{2}} \sum_{r=1}^{N_{\text{perm}}} (-1)^{p_r} \hat{P}_r \hat{Q}_r , \quad (20)$$

where the sum is over all permutations ($N_{\text{perm}} = n_{\text{el}}!$), p_r is the parity (odd or even) of the permutation r , and \hat{P}_r and \hat{Q}_r are the permutation operators acting on the spatial (\mathbf{r}) and the spin ($\boldsymbol{\sigma}$) degrees of freedom, respectively. We note the quasi-idempotency of the antisymmetrizer, $\hat{\mathcal{A}}^2 = (N_{\text{perm}})^{\frac{1}{2}} \hat{\mathcal{A}}$.

Regarding the spin function $\chi_\mu^{(SM_S)} = \chi^{(SM_S)}(\boldsymbol{\theta}_\mu)$, S is the total electron spin quantum number and M_S is the quantum number for the spin projection. S , M_S and the n_{el} define a degenerate spin space in which the spin functions can be expressed by a linear combination (with a linear so-called θ -parameterization) of the elementary spin functions (Supporting Information). The norm of the parameter vector is fixed to 1, thereby reducing the number of free parameters of the spin space. In the non-relativistic energy minimization, we also include the $\boldsymbol{\theta}_\mu$ parameter vector.

Next, let us consider a general, permutationally invariant operator written as a linear combination (in terms of electronic and Cartesian indexes) of products of \hat{G}_{ia} spatial and \hat{T}_{ia} spin-dependent factors,

$$\hat{\mathcal{H}} = \sum_{i=1}^{n_{\text{el}}} \sum_{a=1}^3 \hat{G}_{ia} \hat{T}_{ia} . \quad (21)$$

We compute matrix elements of this operator with non-relativistic electronic functions, $\varphi = \varphi^{(\Gamma, SM_S)}$ and $\varphi' = \varphi^{(\Gamma', S' M'_S)}$ as

$$\begin{aligned} \langle \varphi | \hat{\mathcal{H}} | \varphi' \rangle &= \sum_{\mu=1}^N \sum_{\nu=1}^{N'} C_\mu^* C'_\nu \langle \phi_\mu | \hat{\mathcal{H}} | \phi'_\nu \rangle \\ &= \sum_{\mu=1}^N \sum_{\nu=1}^{N'} C_\mu^* C'_\nu \langle \hat{\mathcal{A}}\{f_\mu \chi_\mu\} | \hat{\mathcal{H}} | \hat{\mathcal{A}}\{f'_\nu \chi'_\nu\} \rangle \\ &= \sum_{\mu=1}^N \sum_{\nu=1}^{N'} C_\mu^* C'_\nu \sum_{r=1}^{N_{\text{perm}}} (-1)^{p_r} \langle f_\mu \chi_\mu | \hat{\mathcal{H}} | (\hat{P}_r f'_\nu)(\hat{Q}_r \chi'_\nu) \rangle \\ &= \sum_{\mu=1}^N \sum_{\nu=1}^{N'} C_\mu^* C'_\nu \sum_{r=1}^{N_{\text{perm}}} (-1)^{p_r} \sum_{i=1}^{n_{\text{el}}} \sum_{a=1}^3 \langle f_\mu | \hat{G}_{ia} | \hat{P}_r f'_\nu \rangle_r \langle \chi_\mu | \hat{T}_{ia} | \hat{Q}_r \chi'_\nu \rangle_\sigma . \end{aligned} \quad (22)$$

The irreducible representation of spatial symmetry can differ for f_μ and f'_ν , hence, the spatial-symmetry operations are retained in the bra and the ket functions. For the computation of the spin-orbit (SO), the spin-own-orbit (SOO),

and the spin-other-orbit (SOO') terms, Eqs. (7)–(9), the \hat{G}_{ia} factors are

$$\text{SO} : \quad \hat{G}_{ia}^{\text{SO}} = \frac{1}{2} \sum_{A=1}^{N_{\text{nuc}}} \frac{Z_A}{r_{iA}^3} \hat{l}_{iA,a} , \quad (23)$$

$$\text{SOO} : \quad \hat{G}_{ia}^{\text{SOO}} = -\frac{1}{2} \sum_{j>i}^{n_{\text{el}}} \frac{1}{r_{ij}^3} \hat{l}_{ij,a} , \quad (24)$$

$$\text{SOO}' : \quad \hat{G}_{ia}^{\text{SOO}'} = -\sum_{j>i}^{n_{\text{el}}} \frac{1}{r_{ij}^3} \hat{l}_{ji,a} , \quad (25)$$

and the \hat{T}_{ia} factor is simply the spin matrix,

$$\hat{T}_{ia} = \hat{s}_{ia} . \quad (26)$$

The spin-spin dipolar term, Eq. (11), is a two-electron term, and by analogous calculation to Eq. (22), we obtain

$$\langle \varphi | \hat{H}_{\text{SS,dp}} | \varphi' \rangle = \sum_{\mu=1}^N \sum_{\nu=1}^{N'} C_{\mu}^* C_{\nu}' \sum_{r=1}^{N_{\text{perm}}} (-1)^{p_r} \sum_{i,j=1}^{n_{\text{el}}} \sum_{a,b=1}^3 \langle f_{\mu} | \hat{G}_{ij,ab} | \hat{P}_r f_{\nu}' \rangle_{\mathbf{r}} \langle \chi_{\mu} | \hat{s}_{ia} \hat{s}_{jb} | \hat{Q}_r \chi_{\nu}' \rangle_{\sigma} . \quad (27)$$

The spatial integrals are calculated analytically by exploiting the mathematical properties of fECGs, similarly to our previous work, *e.g.*, Ref. [17, 20, 53–55].

Since the present work is about the evaluation of the spin-dependent Breit-Pauli matrix elements, some notes regarding the spinor structure and matrix elements are appropriate. To evaluate the spin matrix elements, the spin-adapted ‘ θ ’ parametrization (see also Refs. 56 and 46) is transformed into the spinor (vector) representation (Supporting Information),

$$|\chi^{(SM_S)}(\theta)\rangle = \sum_{\substack{m_{s_1}, m_{s_2}, \dots, m_{s_{n_{\text{el}}}} \\ \Sigma m_{s_i} = M_S}} d_{m_{s_1} m_{s_2} \dots m_{s_{n_{\text{el}}}}^{(SM_S)} |\Xi_{m_{s_1} m_{s_2} \dots m_{s_{n_{\text{el}}}}}\rangle , \quad (28)$$

where $|\Xi_{m_{s_1} m_{s_2} \dots m_{s_{n_{\text{el}}}}}\rangle = |\eta_{m_{s_1}}\rangle \otimes |\eta_{m_{s_2}}\rangle \otimes \dots \otimes |\eta_{m_{s_{n_{\text{el}}}}}\rangle$, and $|\eta_{s_i}\rangle$ is a single-particle spin function (vector). Depending on the $m_{s_i} = -\frac{1}{2}$ or $+\frac{1}{2}$ value, the spin function is ‘spin up’, $|\eta_0\rangle = |\alpha\rangle = \begin{pmatrix} 1 \\ 0 \end{pmatrix}$, or ‘spin down’, $|\eta_1\rangle = |\beta\rangle = \begin{pmatrix} 0 \\ 1 \end{pmatrix}$.

Then, the \hat{s}_i spin operator is considered as the tensor product of identity matrices and the Pauli matrix,

$$\mathbf{s}_{ia} = \frac{\hbar}{2} \mathbf{I}(1) \otimes \mathbf{I}(2) \dots \mathbf{I}(i-1) \otimes \boldsymbol{\sigma}_a(i) \otimes \mathbf{I}(i+1) \dots \otimes \mathbf{I}(n_{\text{el}}) . \quad (29)$$

The matrix representation of the $\hat{s}_{ia} \hat{s}_{jb}$ operator is obtained as $\mathbf{s}_{ia} \mathbf{s}_{jb}$ (the spin space is complete), and

$$\mathbf{s}_{ia} \mathbf{s}_{jb} = \frac{\hbar}{2} \mathbf{I}(1) \otimes \dots \otimes \boldsymbol{\sigma}_a(i) \otimes \dots \otimes \boldsymbol{\sigma}_b(j) \otimes \dots \otimes \mathbf{I}(n_{\text{el}}) , \quad i \neq j \quad (30)$$

$$\mathbf{s}_{ia} \mathbf{s}_{ib} = \frac{\hbar}{2} \mathbf{I}(1) \otimes \dots \otimes \boldsymbol{\sigma}_a \boldsymbol{\sigma}_b(i) \otimes \dots \otimes \mathbf{I}(n_{\text{el}}) . \quad (31)$$

Then, the matrix elements of the spin functions is written as (where the tensor structure can be further exploited)

$$\langle \chi_{\mu} | \hat{s}_{ia} | \chi_{\nu}' \rangle_{\sigma} = \langle \chi_{\mu}^{(SM_S)} | \hat{s}_{ia} | \chi_{\nu}^{(S'M'_S)} \rangle_{\sigma} = \mathbf{d}_{\mu}^{(SM_S)\dagger} \mathbf{s}_{ia} \mathbf{d}_{\nu}^{(S'M'_S)} , \quad (32)$$

$$\langle \chi_{\mu} | \hat{s}_{ia} \hat{s}_{jb} | \chi_{\nu}' \rangle_{\sigma} = \langle \chi_{\mu}^{(SM_S)} | \hat{s}_{ia} \hat{s}_{jb} | \chi_{\nu}^{(S'M'_S)} \rangle_{\sigma} = \mathbf{d}_{\mu}^{(SM_S)\dagger} \mathbf{s}_{ia} \mathbf{s}_{jb} \mathbf{d}_{\nu}^{(S'M'_S)} . \quad (33)$$

In a nutshell, the following algorithm has been implemented in our in-house developed fECG-based computer program, named QUANTEN, to compute matrix elements of spin-dependent relativistic operators connecting various electronic-spin states of small molecules (and also to atoms, of course):

1. The non-relativistic energies and wave functions are determined by the non-linear optimization of the \mathbf{A}_{μ} , \mathbf{s}_{μ} , and $\boldsymbol{\theta}_{\mu}$ parameters and diagonalization of the Hamiltonian for a specific spin state, *e.g.*, $M_S = 0$.

2. The spin function $\chi_\mu^{(SM_S)}$ with parameters θ_μ are transformed to the spinor (vector) representation, Eq. (28), to obtain the $d_{\mathbf{a},\mu}^{(SM_S)}$ coefficients.
3. The spin operators (matrices) \mathbf{s}_i are constructed according to Eq. (29), and the ladder operators (matrices) are generated,

$$\mathbf{s}_i^\pm = \mathbf{s}_{i,x} \pm i\mathbf{s}_{i,y}, \quad \mathbf{S}^\pm = \sum_{i=1}^{n_{\text{el}}} \mathbf{s}_i^\pm, \quad (34)$$

$$(35)$$

Then, the target M_S states are obtained by matrix-vector multiplication,

$$\mathbf{d}_\mu^{(S,M_S\pm 1)} = \mathbf{S}^\pm \mathbf{d}_\mu^{(SM_S)}. \quad (36)$$

4. The spatial matrix elements, $\langle f_\mu^{(\Gamma)} | \hat{G}_{ia}^{\text{rx}} | \hat{P}_r f_\nu^{(\Gamma')} \rangle_{\mathbf{r}}$ ($\text{x}=\text{SO}, \text{SOO}, \text{SOO}'$) and $\langle f_\mu^{(\Gamma)} | \hat{G}_{ij,ab}^{\text{SS}} | \hat{P}_r f_\nu^{(\Gamma')} \rangle_{\mathbf{r}}$ (SS,dp), are computed using the analytic fECG integral expressions.
5. The spatial and spin contributions are combined according to Eqs. (22) and (27), to construct the relativistic (and QED) corrections (coupling matrix elements of the electron-spin states).

IV. NUMERICAL TESTS OF THE IMPLEMENTATION

This section presents numerical examples used to test the computer implementation of the spin-dependent Breit-Pauli Hamiltonian (BP) matrix elements. For the (atomic) test systems, relatively small basis sets are used, which can be readily extended for better-converged results. The value $\alpha^{-1} = 137.035\,999\,177$, recommended by CODATA 2022 [57], is used in all computations.

A. Atomic test system

For the spherically symmetric (atomic) case, high-accuracy ECG implementations are already available [33–35]. As a first test case of our implementation, intended for the more general molecular problem, we computed the spin-dependent BP matrix elements of the 2^3P^o state of the Be atom. We computed the expectation value of the spin-dependent BP operator terms, Eq. (14), labelled as $\langle \hat{H}_X \rangle_J$ ($X = \text{SO}, \text{SOO}, \text{SOO}'$, SS,dp) with the $M_J = 0$ wave function (Table I). The relative error due to the finite basis size is approximately the same for all three terms; the deviations from the reference values are attributed to the incompleteness of our basis set. We also note that the expectation value for other $M_J = \pm 1, \pm 2$ values for 3P states can be calculated through the identities [34],

$$\langle \hat{H}_Y \rangle_0 = 2\langle \hat{H}_Y \rangle_{\pm 1} = -2\langle \hat{H}_Y \rangle_{\pm 2} \quad (37)$$

$$\langle \hat{H}_{\text{SS}} \rangle_0 = -2\langle \hat{H}_{\text{SS}} \rangle_{\pm 1} = 10\langle \hat{H}_{\text{SS}} \rangle_{\pm 2}, \quad (38)$$

where $Y = \text{SO}, \text{SOO}, \text{SOO}'$.

B. Molecular applications

Regarding molecular systems, we are not aware of any literature data for the high-precision computation of the spin-dependent BP matrix elements. Still, to be able to test the spin-dependent BP implementation reported in this work, we used the in-house implementation of the high-precision no-pair Dirac–Coulomb–Breit (DCB) approach [20, 21, 38, 53, 54, 58]. In particular, Ref. [38] is most relevant to this work. For the positive-energy projection, we employed the ‘cutting’ projector [54] and utilised quadruple precision arithmetic operations. The no-pair DCB approach is currently available only for two-electron systems; however, for two-electron triplet di- and triatomic systems, there is a non-vanishing contribution, which is used as a test case. The no-pair DCB energy includes not only the leading-order but also high-order $(Z\alpha)^n$ contributions; but, for small Z nuclear charges, these higher-order contributions are small (so, we did not perform any ‘ α ’ scaling of the variational result [20, 54, 59]).

TABLE I. Be 2^3P^o state: testing the implementation of the spin-dependent Breit–Pauli matrix elements. The non-relativistic energy, $E^{(0)}$ in E_h , and the expectation value of spin-dependent operators for the $M_J = 0$ state in μE_h , are given as a function of the number of ECG functions, N_b .

N_b	$E^{(0)}$	$\alpha^2 \langle \hat{H}_{SO} \rangle_0$	$\alpha^2 \langle \hat{H}_{SOO} + \hat{H}_{SOO'} \rangle_0$	$\alpha^2 \langle \hat{H}_{SS,dp} \rangle_0$
5	-14.44	-24	17.8	1.337
10	-14.54	-28	20.6	1.363
20	-14.553	-30.4	21.76	1.439
30	-14.561 2	-31.60	22.14 1	1.378
50	-14.565 14	-32.06	22.28 8	1.372
100	-14.566 69	-32.18	22.27 8	1.367
Ref. [35]	-14.567 244 230	-32.24 16	22.24 50	1.365

a. Triplet H_2 Two low-energy triplet states of the H_2 molecule are labelled as The a $^3\Sigma_g^+$ and b $^3\Sigma_u^+$. For these states, only the spin-spin matrix elements are non-zero due to spatial symmetry (Table II). The spin-spin interaction lifts the threefold degeneracy of each state, resulting the $\Delta E^{(2)} = E_0^{(2)} - E_{\pm 1}^{(2)}$ zero-field splitting, where the subscript of the energy label the electron spin angular momentum projection on the body-fixed z axis, fixed to the two nuclei. Spin-dependent BP computations in the literature used the Full Configuration Interaction (FCI) approach reaching 1 mE_h convergence of the non-relativistic energy [60]. In the present work, we converged the non-relativistic energy with fECGs to 1 μE_h . The computed $\Delta E^{(2)}$ energy splitting agrees with the literature value (precise to 1-2 digits), but our value is more precise (to 3-4 digits). Furthermore, our perturbative BP energy splitting is in excellent agreement with the no-pair DCB splitting. The no-pair DCB energy was computed using the same fECG parameterisation as the perturbative computations, and not surprisingly, the two energy splittings converge at a similar pace. Differences appear only at the sub- nE_h ($< 10^{-9} E_h$) level, which is well below the finite basis size error (and the range of the leading-order, $\alpha^2 E_h$ relativistic effects).

TABLE II. H_2 a $^3\Sigma_g^+$ and b $^3\Sigma_u^+$ states ($R = 1.4$ bohr): the non-relativistic energy, $E^{(0)}$ in E_h , and the zero-field splitting, ΔE in μE_h . For the perturbative correction $\Delta E^{BP} = \alpha^2 \Delta E^{(2)} = \alpha^2 [E_0^{(2)} - E_{\pm 1}^{(2)}] = \alpha^2 [\langle H_{SS,dp} \rangle_0 - \langle H_{SS,dp} \rangle_{\pm 1}]$ as a function of the number of fECGs, N_b . DCB superscript labels the no-pair DCB computations.

N_b	H_2 a $^3\Sigma_g^+$			H_2 b $^3\Sigma_u^+$		
	$E^{(0)}$	ΔE^{BP}	ΔE^{DCB}	$E^{(0)}$	ΔE^{BP}	ΔE^{DCB}
10	-0.713 250	-0.006 1	-0.006 1	-0.781 5	3.16	3.16
20	-0.713 553	0.013 9	0.013 9	-0.783 3	3.13	3.13
30	-0.713 602	0.019 9	0.019 9	-0.784 121	3.040 3	3.040 2
50	-0.713 635	0.021 45	0.021 45	-0.784 227	3.032 9	3.032 9
100	-0.713 640 21	0.022 31	0.022 31	-0.784 243 5	3.031 09	3.031 05
150	-0.713 640 46	0.022 345	0.022 345	-0.784 244 14	3.030 89	3.030 84
Ref. [60]	-0.713 0	0.02		-0.784 0	3.056	

b. Triplet H_3^+ For the lowest-energy triplet state of H_3^+ , two nuclear geometries are considered (Table III). Previous FCI computations [61, 62] converged the non-relativistic to 10–100 μE_h , but we are not aware of any spin-dependent BP computations and zero-field splitting values published in the literature.

We report computations using the spin-dependent BP implementation (presented in this work) and verify the results against our existing no-pair DCB approach at two distinct nuclear structures. First, we consider the equilibrium structure, which is linear and has two proton-proton distances equal to $R_{pp,1} = R_{pp,2} = 2.454$ bohr [61]. Due to the triatomic, linear geometry, the threefold degeneracy of the energy is lifted into a non-degenerate and a doubly degenerate pair of states with $M_S = 0$ and $M_S = \pm 1$ (where we chose the axis defined by the three nuclei for the quantization axis for the electron spin). Next, we repeated the computation for another, non-linear geometry (which is near a saddle point [62] on the potential energy surface) with two proton-proton distances, $R_{pp,1} = 1.939$ bohr, $R_{pp,2} = 5.961$ bohr, and one proton-proton-proton angle $\angle_{ppp} = 64.4^\circ$. In this case, the three-fold degeneracy of the energy is completely lifted; so, we report two energy splittings for the three energy levels in Table III. The spin-dependent BP implementation is in excellent agreement with the results of the no-pair DCB approach. The latter is

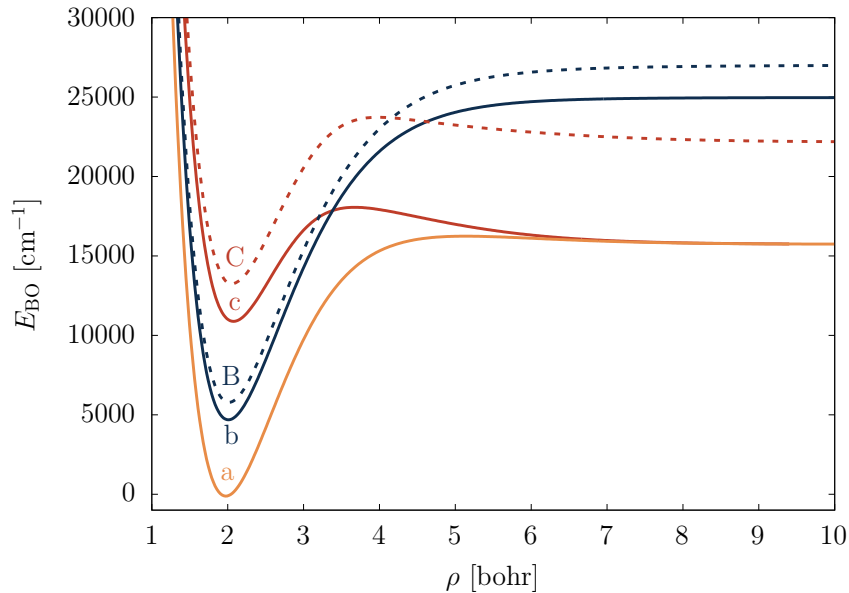


FIG. 1. The low-lying excited triplet and singlet states of He₂ studied in this work.

currently applicable only for two-electron systems, so we proceed with the BP implementation for further molecular applications.

TABLE III. Triplet H₃⁺ ground state: the non-relativistic energy, $E^{(0)}$ in E_h , and the zero-field splitting, ΔE in μE_h , as a function of the number of fECGs, N_b . For linear (equilibrium) structure with centres of fECGs restricted to nuclear axis, $R_{pp,1} = R_{pp,2} = 2.454$ bohr. For the general triangular structure the centers of the ECGs is restricted on the plane of the triangle and no projections are required, $R_{pp,1} = 1.939$ bohr, $R_{pp,2} = 5.961$ bohr, and $\angle_{ppp} = 64.4^\circ$. For the equilibrium geometry, $\Delta E = E_0 - E_{\pm 1} = \alpha^2[\langle \hat{H}_{SS,dp} \rangle_0 - \langle \hat{H}_{SS,dp} \rangle_{\pm 1}]$. For the triangular structure, $\Delta E_{ij} = E_i - E_j$, where i and j labels the energy levels (please see also text). The DCB superscript labels the no-pair Dirac-Coulomb-Breit computation.

N_b	Linear (equilibrium) structure			Triangular structure				
	$E^{(0)}$	ΔE^{BP}	ΔE^{DCB}	$E^{(0)}$	ΔE_{21}^{BP}	ΔE_{21}^{DCB}	ΔE_{32}^{BP}	ΔE_{32}^{DCB}
10	-1.112 7	1.781	1.781	-1.097	0.005 1	0.005 1	0.460 2	0.460 1
20	-1.115 55	1.794	1.794	-1.102 6	0.006 3	0.006 3	0.459 56	0.459 54
30	-1.115 96	1.758 0	1.758 0	-1.103 9	0.006 9	0.006 9	0.459 55	0.459 53
50	-1.116 086	1.757 19	1.757 23	-1.104 29	0.007 4	0.007 4	0.459 35	0.459 33
70	-1.116 102 7	1.757 36	1.757 29	-1.104 36	0.007 63	0.007 63	0.459 25	0.459 23
100	-1.116 107 6	1.756 93	1.756 86	-1.104 391	0.007 79	0.007 79	0.459 152	0.459 132
150	-1.116 108 8	1.756 80	1.757 12	-1.104 402 3	0.007 871	0.007 871	0.459 108	0.459 086
200	-1.116 109 12	1.756 72	1.756 65	-1.104 405 5	0.007 878	0.007 878	0.459 097	0.459 075
Ref.	-1.116 106 3 [61]			-1.104 08 [62]				

V. NUMERICAL APPLICATIONS: HELIUM DIMER

We compute the spin-dependent Breit-Pauli matrix elements connecting electronically excited states of the triplet He₂ molecule (Fig. 1). The convergence of the non-relativistic energy at $\rho = 2$ bohr is reiterated in Table IV, the a $^3\Sigma_u^+$ state taken from Ref. [46] and the b $^3\Pi_g$ and c $^3\Sigma_g^+$ states taken from Ref. [47]. The B $^1\Pi_g$ and C $^1\Sigma_g^+$ states are computed in this work in order to account for the most important relativistic couplings of the a,b,c subspace. The electronic energy was converged by variational (non-linear) optimisation of the fECG basis functions using the stochastic variational method in combination with the Powell non-linear optimizer [9, 10, 46, 63].

In what follows, the atomic nuclei are along the (body-fixed) z axis. The z projection of the total, orbital plus electron spin, angular momentum, $\hat{J}_z = \hat{L}_z + \hat{S}_z$ is conserved for clamped nuclei, and its quantum number is labelled with Ω according to the spectroscopic practice [64]. Application of these results in rovibrational and rovibronic

TABLE IV. Triplet He₂ at $\rho = 2$ bohr: convergence of the non-relativistic energy, $E_x^{(0)}$ in E_h , with respect to the number of optimised fECGs, N_x , for the $x = a, b, c, B,$ and C electronic states (Fig. 1). The ‘a’ state basis set is from Ref. [46], the ‘b’ and ‘c’ states are from Ref. [47].

a $^3\Sigma_u^+$		b $^3\Pi_g$		c $^3\Sigma_g^+$		B $^1\Pi_g$		C $^1\Sigma_g^+$	
N_a	E_a	N_b	E_b	N_c	E_c	N_B	E_B	N_C	E_C
50	-5.146 7	50	-5.124 2	50	-5.092 0	300	-5.124 27	300	-5.089 38
100	-5.149 96	100	-5.127 87	100	-5.097 6	500	-5.124 38	500	-5.089 739
200	-5.150 79	200	-5.128 822	300	-5.100 00			750	-5.089 804
500	-5.151 071	300	-5.128 823	500	-5.100 315				
1000	-5.151 114	500	-5.129 246	750	-5.100 426				
1500	-5.151 122 5	750	-5.129 307	1000	-5.100 465				
2000	-5.151 123 8	1000	-5.129 330	1500	-5.100 482				

computations is reported in Ref. [47] and also in Ref. [46].

In the rest of this section, we report the computation of the relativistic (QED) coupling terms and extensively test their convergence with the basis set size. Comparison with earlier computations by Yarkony [41] is also shown, although the earlier literature results are not well-converged.

A. Fine structure of the a $^3\Sigma_u^+$ state

The lowest-energy triplet state of the He₂ molecule is the a $^3\Sigma_u^+$ state. The relativistic magnetic dipole-dipole interaction, Eq. (11), lifts the threefold degeneracy of this state by splitting it into components with $\Omega = 0$ and $\Omega = \pm 1$ (Fig. 2). This splitting can be characterized by a single parameter, κ , which is the energy deviation of the $\Omega = 0$ state from the centroid. The corresponding shift of the $\Omega = \pm 1$ states is $-\frac{\kappa}{2}$, so the weighted average of the energies equals the centroid energy. The parameter κ has relativistic and QED contributions,

$$\kappa = \alpha^2 \kappa^{(2)} + \alpha^3 \kappa^{(3)}. \quad (39)$$

Since $\kappa^{(2)}$ originates solely from the relativistic magnetic dipole term (SS,dp), Eq. (11), its QED correction is obtained by simple multiplication, Eq. (15),

$$\kappa^{(3)} = \frac{1}{\pi} \kappa^{(2)}. \quad (40)$$

For the a $^3\Sigma_u^+$ state, we think that the non-relativistic energy is converged to 1–10 μE_h for the largest basis sets at $\rho = 2$ bohr internuclear distance (Table IV). The convergence of $\kappa^{(2)}$ with respect to the number of basis functions is shown in Table VI. For the largest basis sets ($N_a = 1000$ – 2000), its value is converged to at least three significant digits. These results agree to one(-two) digit(s) of the Multireference Configuration Interaction (MRCI) computations reported in the literature [42]. The somewhat lower accuracy of the MRCI results is most probably related to the finite basis set error, which we can significantly improve by considering an explicitly correlated basis set.

The A $^1\Sigma_g^+$ state is closest to ‘a’ near equilibrium (Fig. 1), but there is no direct (first-order) coupling between a and A states through the relativistic (and QED) operators, Eqs. (16). Well, they can couple through second-order effects (some details are collected in the Supporting Information), exploratory computations show that these $\alpha^4 E_h$ order contributions are tiny (on the few pico-Hartree, pE_h level), so the A state is not considered further in this work.

B. Fine structure of the b $^3\Pi_g$ and c $^3\Sigma_g^+$ states

The non-vanishing spin-dependent BP matrix elements connecting the b and c states are collected in Table V. The parameter ε labels the separation (zero-field splitting) of the $M_S = 0$ and $M_S = \pm 1$ states in the c subspace. For the b subspace, the non-zero electron orbital angular momentum introduces a more complicated splitting pattern. It takes three independent parameters, labelled as β , γ_1 , and γ_2 , which describe the shift and splitting of the originally six-fold degenerate subspace into three two-fold degenerate states with $\Omega = \pm 2$, $\Omega = \pm 1$, and $\Omega = 0$ (Fig. 2).

Additionally, the b and c electronic-spin states couple through the matrix elements labelled as δ_1 and δ_2 in Table VI, hence, only the b states for $\Omega = \pm 2$ remain degenerate.

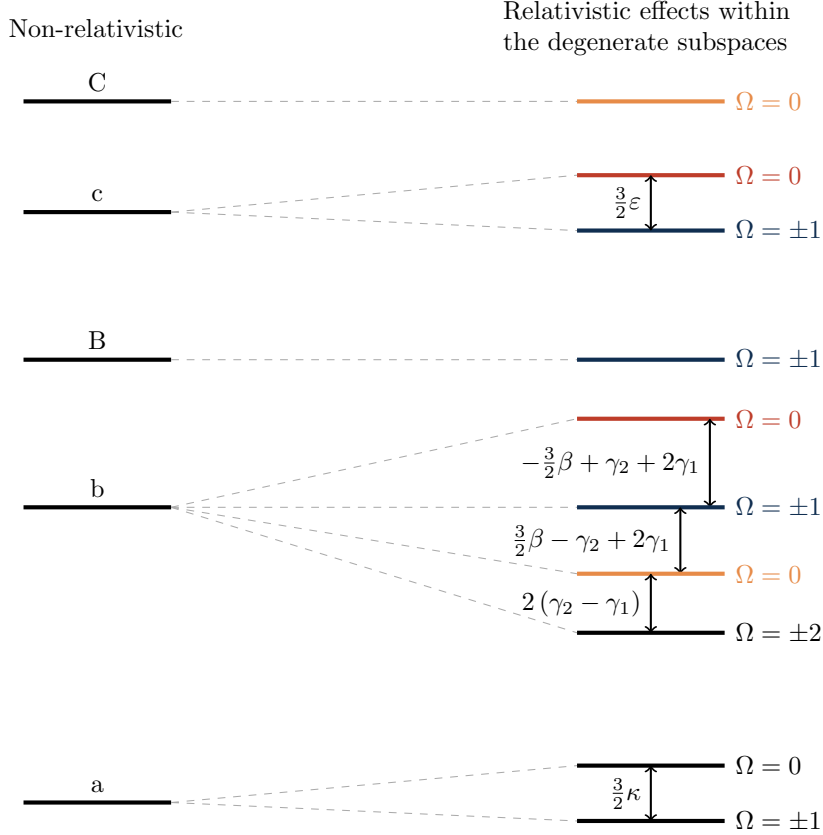


FIG. 2. Triplet He_2 : Splitting of the non-relativistic energies degenerate in M_S by spin-dependent relativistic (and QED) terms. For the definition of λ , δ_1 , δ_2 , ζ , and ξ please see Table VI (and Ref. [47]). The colors indicate states, which couples with each other through relativistic interactions (red - λ , purple - δ_2 , green - δ_1, ζ, ξ).

Non-negligible couplings also exist with the singlet states, most importantly, with the B $^1\Pi_g$ and the C $^1\Sigma_g^+$ states (Fig. 1); the non-vanishing BP matrix elements are with λ , ζ , and ξ in Table V. The computations of these matrix elements require all together about 500 CPU hours for the largest basis sets. Similarly to κ , the relativistic and QED couplings for the parameters β , γ_1 , and ϵ differ only by a simple multiplicative factor, since only the magnetic dipole term contributes to the relativistic coupling,

$$\beta^{(3)} = \frac{1}{\pi}\beta^{(2)}, \quad \gamma_1^{(3)} = \frac{1}{\pi}\gamma_1^{(2)}, \quad \epsilon^{(3)} = \frac{1}{\pi}\epsilon^{(2)}. \quad (41)$$

For the other matrix elements, the QED terms were calculated according to Eq. (15), and their convergence is shown in Table VII. For matrix elements with the singlet B and C states, due to the smaller basis sets used in this work, the non-relativistic energies are by 1-2 orders of magnitude less accurate than the a non-relativistic energy (Table IV). Despite this lower accuracy, the precision of the relativistic and QED couplings appears to be comparable to that of κ , the uncertainties are in the second digit after the decimal point (Tables VI and VII). To test the convergence, we increased the B and C basis sizes to $N_B = 500$ and $N_C = 750$, respectively, while using the largest b and c basis sets. The resulting changes in the coupling values are in the 2nd to the 4th digits. These results are expected to be sufficiently accurate for the rovibronic computations, primarily focusing on b-c states, as presented in Ref. [47].

VI. SUMMARY, CONCLUSION, AND OUTLOOK

In this paper, we reported methodological details and benchmark numerical results for the spin-dependent relativistic and leading-order QED couplings of electronic states of small molecules. The relativistic and QED couplings of the high-precision non-relativistic electronic states are computed as matrix elements of the spin-dependent operators of the Breit-Pauli Hamiltonian, including the spin-orbit, spin-own-orbit, spin-other-orbit, and spin-spin terms. The

TABLE V. Non-vanishing spin-dependent relativistic (and QED) matrix elements within the b, c, B, C electronic-spin subspace of He₂. The superscript of each state labels the Cartesian component of the spatial part (as computed in QUANTEN) and the M_S quantum number of the total electron-spin projection on the internuclear axis. The ‘.’ labels zero (0).

	$b^{x,-1}$	$b^{x,0}$	$b^{x,1}$	$b^{y,-1}$	$b^{y,0}$	$b^{y,1}$	$c^{0,-1}$	$c^{0,0}$	$c^{0,1}$	$B^{x,0}$	$B^{y,0}$	$C^{0,0}$
$b^{x,-1}$	$-\beta$.	$-\gamma_1$	$-i\gamma_2$.	$-i\gamma_1$.	δ_2	.	.	.	λ
$b^{x,0}$.	2β	$-\delta_1$.	δ_1	.	$i\zeta$.
$b^{x,1}$	$-\gamma_1$.	$-\beta$	$i\gamma_1$.	$i\gamma_2$.	$-\delta_2$.	.	.	λ
$b^{y,-1}$	$i\gamma_2$.	$-i\gamma_1$	$-\beta$.	γ_1	.	$i\delta_2$.	.	.	$i\lambda$
$b^{y,0}$	2β	.	$i\delta_1$.	$i\delta_1$	$-i\zeta$.	.
$b^{y,1}$	$i\gamma_1$.	$-i\gamma_2$	γ_1	.	$-\beta$.	$i\delta_2$.	.	.	$-i\lambda$
$c^{0,-1}$.	$-\delta_1$.	.	$-i\delta_1$.	$-\varepsilon$.	.	ξ	$i\xi$.
$c^{0,0}$	δ_2	.	$-\delta_2$	$-i\delta_2$.	$-i\delta_2$.	2ε
$c^{0,1}$.	δ_1	.	.	$-i\delta_1$.	.	.	$-\varepsilon$	ξ	$-i\xi$.
$B^{x,0}$	$i\zeta$.	ξ	.	ξ	.	.	.
$B^{y,0}$.	$-i\zeta$	$-i\xi$.	$i\xi$.	.	.
$C^{0,0}$	λ	.	λ	$-i\lambda$.	$i\lambda$

TABLE VI. Convergence of the relativistic spin-dependent contributions, in mE_h/α^2 , within the a, b, c, B, and C electronic-spin subspace of He₂ at $R = 2.00$ bohr. κ corresponds to the zero-field splitting of the ‘a’ state, and Table V defines all other non-vanishing matrix elements within the b, c, B, C subspace. $N_B = 300$ and $N_C = 500$, unless stated otherwise.

N_a	N_b	N_c	$\kappa^{(2)}$	$\beta^{(2)}$	$\gamma_1^{(2)}$	$\gamma_2^{(2)}$	$\delta_1^{(2)}$	$\delta_2^{(2)}$	$\varepsilon^{(2)}$	$\lambda^{(2)}$	$\zeta^{(2)}$	$\xi^{(2)}$
50	50	50	1.7	-3.19	12.24	20.7	-1.57	-8.68	1.61	-5.735	28.831	10.070
100	100	100	1.9	-3.19	12.43	19.99	-1.24	-8.67	1.65	-5.756	29.606	10.495
200	300	300	2.01	-3.182	12.472	19.69	-1.01	-8.596	1.688	-5.768	29.815	10.764
500	500	500	2.07	-3.1694	12.4671	19.621	-0.931	-8.559	1.6947	-5.768	29.870	10.835
1000	750	750	2.078	-3.1689	12.4691	19.598	-0.914	-8.549	1.6951	-5.764	29.881	10.858
1500	1000	1000	2.081	-3.1687	12.4691	19.586	-0.901	-8.538	1.6946	-5.763	29.883	10.862
2000	1000	1500	2.082	-3.1687	12.4691	19.586	-0.898	-8.537	1.6952	-5.763	29.883	10.866
—	1000	1500 [†]	—	—	—	—	—	—	—	-5.767	29.929	10.874
Musher <i>ℓ</i> <i>co-w.</i> [39]*			2.01	—	—	—	—	—	—	—	—	—
Minaev [43] [◦]			—	—	—	—	—	—	2.14	—	—	—
Yarkony [41]			—	—	—	—	-1.20	-4.39	—	-4.359	24.330	10.375
Rosmus <i>ℓ</i> <i>co-w.</i> [42]			2.107	-3.200	12.552	20.62	—	—	—	—	—	—

[†] : $N_B = 500$ and $N_C = 750$.

* : $R = 2.015$ bohr bond distance for a $^3\Sigma_u^+$.

◦ : $R = 2.08$ bohr bond distance for c $^3\Sigma_g^+$.

TABLE VII. Convergence of the spin-dependent, leading-order QED contributions, in $0.1 mE_h/\alpha^3$, within the b, c, B, and C electronic-spin subspace of He₂ (see also Tables V and VI). $N_B = 300$ and $N_C = 500$, unless stated otherwise. $\beta^{(3)}$, $\gamma_1^{(3)}$, $\varepsilon^{(3)}$, and $\kappa^{(3)}$ can be calculated from Eqs. (40)–(41) and Table VI.

N_b	N_c	$\gamma_2^{(3)}$	$\delta_1^{(3)}$	$\delta_2^{(3)}$	$\lambda^{(3)}$	$\zeta^{(3)}$	$\xi^{(3)}$
50	50	0.28	-1.22	-1.13	1.236	-7.66	2.06
100	100	0.02	-1.24	-0.84	1.250	-7.87	2.15
300	300	0.138	-1.511	-0.91	1.261	-7.94	2.221
500	500	0.160	-1.502	-0.925	1.264	-7.951	2.238
750	750	0.168	-1.500	-0.931	1.2630	-7.9551	2.243
1000	1000	0.171	-1.4974	-0.934	1.2626	-7.9560	2.244
1000	1500	0.171	-1.4966	-0.935	1.2626	-7.9560	2.246
1000	1500 [†]	—	—	—	1.2638	-7.9676	2.2453

[†] : $N_B = 500$ and $N_C = 750$.

corrections due to the electron’s anomalous magnetic moment are also accounted for. To accurately describe small polyelectronic molecules, we use a variational floating explicitly correlated Gaussian (fECG) basis procedure.

For small molecular species, accurate and complete fine-structure data are scarcely available, and this work fills this gap. First of all, we tested the methodology for an atomic system, for which (higher precision) fine-structure splitting data are already available in the literature. Then, we computed spin-dependent Breit-Pauli Hamiltonian matrix elements for the two-electron triplet H_2 and triplet H_3^+ . High-precision literature data are not available for these fine-structure splittings; however, for these two-electron systems, we verified the results against our in-house developed no-pair Dirac-Coulomb-Breit (np-DCB) Hamiltonian approach, using the same fECG spatial basis set in the two computations. The two approaches give identical splittings to high precision (the most stringent, direct comparison would be possible by α -scaling the np-DCB results and comparing the $\alpha^2 E_h$ order term).

The spin-dependent Breit-Pauli Hamiltonian matrix elements can be evaluated for (in principle) general polyelectronic and poly-atomic molecules, whereas our current np-DCB ECG implementation is for two electrons (but automatically includes higher-order $(Z\alpha)^n$ effects).

As to new numerical results with the developed methodology, we converge the relativistic and QED couplings for electronically excited triplet (a $^3\Sigma_u^+$, b $^3\Pi_g$, and c $^3\Sigma_g^+$) and singlet (B $^1\Pi_g$, C $^1\Sigma_g^+$) states of the four-electron He_2 molecule to at least 3-4 significant digits, which significantly improves upon (the scarcely) available data in the literature. These results are computed for a series of nuclear configurations and will be used to compute high-resolution spectra, including modelling the fine structure of the rovibronic transitions in a separate paper.

ACKNOWLEDGEMENT

PJ gratefully acknowledges the support of the János Bolyai Research Scholarship of the Hungarian Academy of Sciences (BO/285/22). We thank the European Research Council (Award No. 851421) and the Momentum Programme of the Hungarian Academy of Sciences (LP2024-15/2024) for their financial support. We acknowledge KIFÜ (Governmental Agency for IT Development, Hungary) for access to the Komondor HPC facility based in Hungary.

-
- [1] R. E. Sheldon, T. J. Babij, S. H. Reeder, S. D. Hogan, and D. B. Cassidy, Precision microwave spectroscopy of the positronium $2\ ^3S_1 \rightarrow 2\ ^3P_2$ interval, *Phys. Rev. Lett.* **131**, 043001 (2023).
 - [2] G. Clausen, S. Scheidegger, J. A. Agner, H. Schmutz, and F. Merkt, Imaging-Assisted Single-Photon Doppler-Free Laser Spectroscopy and the Ionization Energy of Metastable Triplet Helium, *Phys. Rev. Lett.* **131**, 103001 (2023).
 - [3] S. Alighanbari, G. S. Giri, F. L. Constantin, V. I. Korobov, and S. Schiller, Precise test of quantum electrodynamics and determination of fundamental constants with HD^+ ions, *Nature* **581**, 152 (2020).
 - [4] S. Patra, M. Germann, J.-P. Karr, M. Haidar, L. Hilico, V. I. Korobov, F. M. J. Cozijn, K. S. E. Eikema, W. Ubachs, and J. C. J. Koelemeij, Proton-electron mass ratio from laser spectroscopy of HD^+ at the part-per-trillion level, *Science* **369**, 1238 (2020).
 - [5] M. Germann, S. Patra, J.-P. Karr, L. Hilico, V. I. Korobov, E. J. Salumbides, K. S. E. Eikema, W. Ubachs, and J. C. J. Koelemeij, Three-body QED test and fifth-force constraint from vibrations and rotations of HD^+ , *Phys. Rev. Res.* **3**, L022028 (2021).
 - [6] T. Langen, G. Valtolina, D. Wang, and J. Ye, Quantum state manipulation and cooling of ultracold molecules, *Nat. Phys.* **20**, 702–712 (2024).
 - [7] B. J. Furey, Z. Wu, M. Isaza-Monsalve, S. Walser, E. Mattivi, R. Nardi, and P. Schindler, Strategies for implementing quantum error correction in molecular rotation, *Quantum* **8**, 1578 (2024).
 - [8] D. K. Ruttley, T. R. Hepworth, A. Guttridge, and S. L. Cornish, Long-lived entanglement of molecules in magic-wavelength optical tweezers, *Nature* **637**, 827–832 (2025).
 - [9] Y. Suzuki and K. Varga, *Stochastic Variational Approach to Quantum-Mechanical Few-Body Problems* (Springer-Verlag, Berlin, 1998).
 - [10] J. Mitroy, S. Bubin, W. Horiuchi, Y. Suzuki, L. Adamowicz, W. Cencek, K. Szalewicz, J. Komasa, D. Blume, and K. Varga, Theory and application of explicitly correlated Gaussians, *Rev. Mod. Phys.* **85**, 693 (2013).
 - [11] K. Strasburger, High angular momentum states of lithium atom, studied with symmetry-projected explicitly correlated gaussian lobe functions, *J. Chem. Phys.* **141**, 044104 (2014).
 - [12] K. Strasburger, Explicitly correlated wave functions of the ground state and the lowest quintuplet state of the carbon atom, *Phys. Rev. A* **99**, 052512 (2019).
 - [13] W. Cencek, Relativistic Calculations Using Explicitly Correlated Gaussian Functions, in *Explicitly Correlated Wave Functions in Chemistry and Physics: Theory and Applications*, edited by J. Rychlewski (Springer Netherlands, Dordrecht, 2003) pp. 347–370.
 - [14] M. Pavanello, L. Adamowicz, A. Alijah, N. F. Zobov, I. I. Mizus, O. L. Polyansky, T. S. J. Tennyson, and A. G. Császár, Calibration-quality adiabatic potential energy surfaces for h_3^+ and its isotopologues, *J. Chem. Phys.* **136**, 184303 (2012).

- [15] W.-C. Tung, M. Pavanello, and L. Adamowicz, Very accurate potential energy curve of the He_2^+ ion, *J. Chem. Phys.* **136**, 104309 (2012).
- [16] D. Ferenc and E. Mátyus, Non-adiabatic mass correction for excited states of molecular hydrogen: Improvement for the outer-well $H\bar{H} \ ^1\Sigma_g^+$ term values, *J. Chem. Phys.* **151**, 094101 (2019).
- [17] D. Ferenc, V. I. Korobov, and E. Mátyus, Nonadiabatic, relativistic, and leading-order QED corrections for rovibrational intervals of $^4\text{He}_2^+$ ($X \ ^2\Sigma_u^+$), *Phys. Rev. Lett.* **125**, 213001 (2020).
- [18] V. Patkóš, V. A. Yerokhin, and K. Pachucki, Complete $\alpha^7 m$ Lamb shift of helium triplet states, *Phys. Rev. A* **103**, 042809 (2021).
- [19] S. Nasiri, D. Tumakov, M. Stanke, A. Kędzioriski, L. Adamowicz, and S. Bubin, Fine structure of the doublet P levels of boron, *Phys. Rev. Res.* **6**, 043225 (2024).
- [20] D. Ferenc, P. Jeszenszki, and E. Matyus, Variational versus perturbative relativistic energies for small and light atomic and molecular systems, *J. Chem. Phys.* **157**, 094113 (2022).
- [21] E. Mátyus, D. Ferenc, P. Jeszenszki, and A. Margócsy, The Bethe–Salpeter QED Wave Equation for Bound-State Computations of Atoms and Molecules, *ACS Phys. Chem Au* **3**, 222 (2023).
- [22] K. Pachucki, W. Cencek, and J. Komasa, On the acceleration of the convergence of singular operators in Gaussian basis sets, *J. Chem. Phys.* **122**, 184101 (2005).
- [23] P. Jeszenszki, R. T. Ireland, D. Ferenc, and E. Mátyus, On the inclusion of cusp effects in expectation values with explicitly correlated Gaussians, *Int. J. Quant. Chem.* **122**, e26819 (2022).
- [24] B. Rácsai, D. Ferenc, A. Margócsy, and E. Mátyus, Regularized relativistic corrections for polyelectronic and polyatomic systems with explicitly correlated Gaussians, *J. Chem. Phys.* **160**, 211102 (2024).
- [25] M. Douglas and N. M. Kroll, Quantum electrodynamical corrections to the fine structure of helium, *Ann. Phys.* **82**, 89 (1974).
- [26] V. c. v. Patkóš, V. A. Yerokhin, and K. Pachucki, Two-body P -state energies at order α^6 , *Phys. Rev. A* **109**, 022819 (2024).
- [27] V. A. Yerokhin, V. c. v. Patkóš, M. Puchalski, and K. Pachucki, QED calculation of ionization energies of $1snd$ states in helium, *Phys. Rev. A* **102**, 012807 (2020).
- [28] V. A. Yerokhin, V. c. v. Patkóš, and K. Pachucki, Atomic structure calculations of helium with correlated exponential functions, *Symmetry* **13**, 1246 (2021).
- [29] S. D. Bergeson, A. Balakrishnan, K. G. H. Baldwin, T. B. Lucatorto, J. P. Marangos, T. J. McIlrath, T. R. O’Brian, S. L. Rolston, C. J. Sansonetti, J. Wen, N. Westbrook, C. H. Cheng, and E. E. Eyler, Measurement of the He Ground State Lamb Shift via the Two-Photon $1 \ ^1s - 2 \ ^1s$ Transition, *Phys. Rev. Lett.* **80**, 3475–3478 (1998).
- [30] D. Z. Kandula, C. Gohle, T. J. Pinkert, W. Ubachs, and K. S. E. Eikema, XUV frequency-comb metrology on the ground state of helium, *Phys. Rev. A* **84**, 062512 (2011).
- [31] G. Clausen, P. Jansen, S. Scheidegger, J. A. Agner, H. Schmutz, and F. Merkt, Ionization Energy of the Metastable $2 \ ^1S_0$ State of ^4He from Rydberg-Series Extrapolation, *Phys. Rev. Lett.* **127**, 093001 (2021).
- [32] G. Clausen and F. Merkt, Ionization Energy of Metastable ^3He ($2 \ ^3S_1$) and the Alpha- and Helion-Particle Charge-Radius Difference from Precision Spectroscopy of the np Rydberg Series, *Phys. Rev. Lett.* **134**, 223001 (2025).
- [33] M. Puchalski, J. Komasa, and K. Pachucki, Fine and hyperfine splitting of the low-lying states of Be^9 , *Phys. Rev. A* **104**, 2469 (2021).
- [34] A. Kędzioriski, M. Stanke, and L. Adamowicz, Atomic fine-structure calculations performed with a finite-nuclear-mass approach and with all-electron explicitly correlated Gaussian functions, *Chem. Phys. Lett.* **751**, 137476 (2020).
- [35] M. Stanke, A. Kędzioriski, and L. Adamowicz, Fine structure of the beryllium 3P states calculated with all-electron explicitly correlated gaussian functions, *Phys. Rev. A* **105**, 012813 (2022).
- [36] V. A. Yerokhin, V. c. v. Patkóš, and K. Pachucki, QED calculations of energy levels of heliumlike ions with $5 \leq Z \leq 30$, *Phys. Rev. A* **106**, 022815 (2022).
- [37] S. Nasiri, S. Bubin, and L. A. and, Isotopic shifts in 3P states of the carbon atom, *Mol. Phys.* **122**, e2325049 (2024).
- [38] P. Jeszenszki and E. Mátyus, Relativistic two-electron atomic and molecular energies using ls coupling and double groups: Role of the triplet contributions to singlet states, *J. Chem. Phys.* **158**, 054104 (2023).
- [39] D. R. Beck, C. A. Nicolaides, and J. I. Musher, Calculation of the fine structure of the $a \ ^3\Sigma_u^+$ state of molecular helium, *Phys. Rev. A* **10**, 1522–1527 (1974).
- [40] C. F. Chabalowski, J. O. Jensen, D. R. Yarkony, and B. H. Lengsfeld, Theoretical study of the radiative lifetime for the spin-forbidden transition $a \ ^3\Sigma_u^+ \rightarrow X \ ^1\Sigma_g^+$ in He_2 , *J. Chem. Phys.* **90**, 2504 (1989).
- [41] D. R. Yarkony, On the quenching of helium $2 \ ^3S$: Potential energy curves for, and nonadiabatic, relativistic, and radiative couplings between, the $a \ ^3\Sigma_u^+$, $A \ ^1\Sigma_u^+$, $b \ ^3\Pi_g$, $B \ ^1\Pi_g$, $c \ ^3\Sigma_g^+$, and $C \ ^1\Sigma_g^+$ states of He_2 , *J. Chem. Phys.* **90**, 7164 (1989).
- [42] N. Bjerre, A. O. Mitrushekov, P. Palmieri, and P. Rosmus, Spin-orbit and spin-spin couplings in He_2 and He_2^- , *Theor. Chem. Acc.* **100**, 51 (1998).
- [43] B. Minaev, Fine structure and radiative lifetime of the low-lying triplet states of the helium excimer, *Phys. Chem. Chem. Phys.* **5**, 2314 (2003).
- [44] P. Nijjar, A. I. Krylov, O. V. Prezhdo, A. F. Vilesov, and C. Wittig, Triplet excitons in small helium clusters, *J. Phys. Chem. A* **123**, 6113–6122 (2019).
- [45] S. Xu, A. Lu, X. Zhong, Y. Guo, and J. Shi, Ab initio investigation of potential energy curves of He_2 , He_2^+ , and extrapolation by the machine learning method, *Int. J. Quant. Chem.* **124**, e27367 (2024).

- [46] Á. Margócsy, B. Rácsai, P. Jeszenszki, and E. Mátyus, Rovibrational computations for the He₂ a ³Σ_u⁺ state including non-adiabatic, relativistic, and QED corrections, (to be submitted).
- [47] B. Rácsai, P. Jeszenszki, Á. Margócsy, and E. Mátyus, High-precision quantum dynamics of He₂ (b ³Π_g-c ³Σ_g⁺) including non-adiabatic, relativistic and QED corrections and couplings, (to be submitted).
- [48] K. G. Dyall and K. Faegri, Jr., *Introduction to Relativistic Quantum Chemistry* (Oxford University Press, New York, 2007).
- [49] M. Reiher and A. Wolf, *Relativistic Quantum Chemistry: The Fundamental Theory of Molecular Science, 2nd edition* (Wiley-VCH, Weinheim, 2015).
- [50] J. Schwinger, On quantum-electrodynamics and the magnetic moment of the electron, *Phys. Rev.* **73**, 416 (1948).
- [51] J. Sucher, Energy levels of the two-electron atom, to order α³ Rydberg (PhD dissertation, Columbia University) (1958).
- [52] U. D. Jentschura and G. S. Adkins, *Quantum Electrodynamics: Atoms, Lasers and Gravity* (World Scientific, Singapore, 2022).
- [53] P. Jeszenszki, D. Ferenc, and E. Mátyus, All-order explicitly correlated relativistic computations for atoms and molecules, *J. Chem. Phys.* **154**, 224110 (2021).
- [54] P. Jeszenszki, D. Ferenc, and E. Mátyus, Variational Dirac–Coulomb explicitly correlated computations for molecules, *J. Chem. Phys.* **156**, 084111 (2022).
- [55] D. Ferenc, P. Jeszenszki, and E. Mátyus, On the Breit interaction in an explicitly correlated variational Dirac–Coulomb framework, *J. Chem. Phys.* **156**, 084110 (2022).
- [56] E. Mátyus and Á. Margócsy, Rovibrational computations for He₂⁺ X⁺ Σ_u⁺ including non-adiabatic, relativistic and QED corrections, (to be submitted).
- [57] P. J. Mohr, D. B. Newell, B. N. Taylor, and E. Tiesinga, CODATA recommended values of the fundamental physical constants: 2022, *Rev. Mod. Phys.* **97**, 025002 (2025).
- [58] P. Hollósy, P. Jeszenszki, and E. Mátyus, One-particle operator representation over two-particle basis sets for relativistic qed computations, *J. Chem. Theory Comput.* **20**, 5122 (2024).
- [59] A. Nonn, A. Margócsy, and E. Mátyus, Bound-State Relativistic Quantum Electrodynamics: A Perspective for Precision Physics with Atoms and Molecules, *J. Chem. Theory Comput.* **20**, 4385 (2024).
- [60] B. Minaev, O. Loboda, Z. Rinkevicius, O. Valtras, and H. Ågren, Fine and hyperfine structure in three low-lying ³Σ⁺ states of molecular hydrogen, *Mol. Phys.* **101**, 2335 (2003).
- [61] C. Sanz, O. Roncero, C. Tablero, A. Aguado, and M. Paniagua, The lowest triplet state A₃⁺ of H₃⁺: Global potential energy surface and vibrational calculations, *J. Chem. Phys.* **114**, 2182 (2001).
- [62] M. Cernei, A. Alijah, and A. J. C. Varandas, Accurate double many-body expansion potential energy surface for triplet H₃⁺. I. The lowest adiabatic sheet (a ³Σ_u⁺), *J. Chem. Phys.* **118**, 2637 (2003).
- [63] E. Mátyus and M. Reiher, Molecular Structure Calculations: a Unified Quantum Mechanical Description of Electrons and Nuclei using Explicitly Correlated Gaussian Functions and the Global Vector Representation, *J. Chem. Phys.* **137**, 024104 (2012).
- [64] H. Lefebvre-Brion and R. W. Field, *The Spectra and Dynamics of Diatomic Molecules* (Academic Press, 2004).
- [65] R. Pauncz, *Spin Eigenfunctions* (Springer, New York, NY, 1979).
- [66] K. Pachucki, Higher-order effective Hamiltonian for light atomic systems, *Phys. Rev. A* **71**, 012503 (2005).
- [67] K. Pachucki and V. A. Yerokhin, Reexamination of the helium fine structure, *Phys. Rev. A* **79**, 062516 (2009).
- [68] I. Shavitt and R. J. Bartlett, *Many-body methods in chemistry and physics: MBPT and coupled-cluster theory*, Cambridge molecular science (Cambridge University Press, Cambridge, England, 2009).
- [69] M. D. E. Epée, O. Motapon, K. Chakrabarti, and J. Tennyson, Theoretical investigation of Rydberg states of He₂ using the *R*-matrix method, *Mol. Phys.* **122**, e2295013 (2024).

Supplemental Material

Spin-dependent terms of the Breit-Pauli Hamiltonian evaluated with explicitly correlated Gaussian basis set for molecular computations

Péter Jeszenszki,¹ Péter Hollósy,¹ Ádám Margócsy,¹ Edit Mátyus^{1,*}

¹ *MTA–ELTE ‘Momentum’ Molecular Quantum electro-Dynamics Research Group, Institute of Chemistry, Eötvös Loránd University, Pázmány Péter sétány 1/A, Budapest, H-1117, Hungary*

* edit.matyus@ttk.elte.hu

(Dated: 23 June 2025)

S1. REPRESENTATION OF THE SPIN FUNCTION WITH SPIN-ADAPTED STATES AND SPINORS - CASE STUDY FOR FOUR PARTICLES WITH $M_S = 0$

The simplest representation of the spin part of the wave function is via spinors, which are basis vectors in \mathbb{C}^{2^N} ,

$$|\Xi_{m_{s_1} m_{s_2} \dots m_{s_{n_{el}}}\rangle} = |\eta_{m_{s_1}}\rangle \otimes |\eta_{m_{s_2}}\rangle \otimes \dots \otimes |\eta_{m_{s_{n_{el}}}}\rangle \quad (\text{S1})$$

where $|\eta_{m_{s_i}}\rangle$ is a single-particle spin function (vector). For $m_{s_i} = -1/2$, the spin function is ‘spin up’,

$$|\eta_0\rangle = |\alpha\rangle = \begin{pmatrix} 1 \\ 0 \end{pmatrix}, \quad (\text{S2})$$

for $m_{s_i} = +1/2$, it is ‘spin down’,

$$|\eta_1\rangle = |\beta\rangle = \begin{pmatrix} 0 \\ 1 \end{pmatrix}. \quad (\text{S3})$$

The $\{|\Xi_{m_{s_1} m_{s_2} \dots m_{s_{n_{el}}}\rangle}\}$ form a basis for spin eigenfunctions (see Ref. [65] and the Supplementary Material of Ref. 46). For four electrons with $M_S = 0$, the spin-adapted states are as follows. We have two singlet ($S = 0$) states,

$$\begin{aligned} |\Theta_{0,0}^{(1)}\rangle &= \frac{1}{\sqrt{12}} (|\Xi_{0011}\rangle - 2|\Xi_{0101}\rangle + |\Xi_{0110}\rangle + |\Xi_{1001}\rangle - 2|\Xi_{1010}\rangle + |\Xi_{1100}\rangle) \\ |\Theta_{0,0}^{(2)}\rangle &= \frac{1}{2} (|\Xi_{0011}\rangle - |\Xi_{0110}\rangle - |\Xi_{1001}\rangle + |\Xi_{1100}\rangle), \end{aligned}$$

three triplet ($S = 1$) states,

$$\begin{aligned} |\Theta_{1,0}^{(1)}\rangle &= \frac{1}{\sqrt{2}} (|\Xi_{0011}\rangle - |\Xi_{1100}\rangle) \\ |\Theta_{1,0}^{(2)}\rangle &= \frac{1}{\sqrt{2}} (|\Xi_{0101}\rangle - |\Xi_{1010}\rangle) \\ |\Theta_{1,0}^{(3)}\rangle &= \frac{1}{\sqrt{2}} (|\Xi_{0110}\rangle - |\Xi_{1001}\rangle). \end{aligned}$$

and one set of quintuplet ($S = 2$) state,

$$|\Theta_{2,0}\rangle = \frac{1}{\sqrt{6}} (|\Xi_{0011}\rangle + |\Xi_{0101}\rangle + |\Xi_{0110}\rangle + |\Xi_{1001}\rangle + |\Xi_{1010}\rangle + |\Xi_{1100}\rangle).$$

Despite this, the spin-adapted implementation becomes complicated for the general N -electron case, especially for the computation of matrix elements with spin-dependent relativistic operators. Therefore, in this work, we have switched to the spinor representation, in which the calculation of spin-dependent operator matrix elements can be more efficiently automated.

For the transformation between the two representations, *i.e.*, the spin-adapted ‘ Θ ’ parameterisation vs. spinor linear

combination, the relation between $C_{k,S}$ and $d_{m_{s_1}, \dots, m_{s_{n_{el}}}}^{(SM_S)}$ is

$$\begin{aligned}
|\chi_{S,M_S}(\boldsymbol{\theta})\rangle &= \sum_{k=1}^{N_s(n_{el},S)} C_{k,S}(\boldsymbol{\theta}) |\Theta_{S,M_S}^{(k)}\rangle, \\
&= \sum_{k=1}^{N_s(n_{el},S)} C_{k,S}(\boldsymbol{\theta}) \sum_{\substack{s_1, \dots, s_{n_{el}} \\ \Sigma s_i = M_S}} Q_{s_1 \dots s_{n_{el}}}^{S,M_S,k} |\Xi_{s_1 s_2 \dots s_{n_{el}}}\rangle \\
&= \sum_{\substack{m_{s_1}, \dots, m_{s_{n_{el}}} \\ \Sigma m_{s_i} = M_S}} d_{m_{s_1}, \dots, m_{s_{n_{el}}}^{(SM_S)}(\boldsymbol{\theta}) |\Xi_{s_1 s_2 \dots s_{n_{el}}}\rangle,
\end{aligned} \tag{S4}$$

and this change of representation is performed in an automated procedure in QUANTEN. For the example of the helium dimer's case, the non-relativistic energy optimisation was performed in the spin-adapted $\boldsymbol{\theta}$ parameterization, which was converted to the spinor representation, which means storing a 2^4 -dimensional vector for every basis function (instead of the 1-2 ϑ parameters). The latter representation can be more straightforwardly used for the evaluation of the spin-dependent BP matrix elements.

Although the non-relativistic wave functions are degenerate in M_S , but we need to generate functions with another M_S value for computing the BP matrix elements. For this purpose, Eq. (S4) and the matrix representation of the spin-ladder operators were employed.

S2. HIGHER-ORDER FINE-STRUCTURE CORRECTIONS FROM OTHER ELECTRONIC STATES

In this section, we examine possible $\alpha^4 E_h$ -order relativistic contributions for close-lying electronic states that can couple through the spin-dependent BP terms. At the same time, we note that a complete treatment of the $\alpha^4 E_h$ correction requires consideration of several QED terms as well [25, 66, 67], which are beyond the scope of this paper.

In the case of closely degenerate states such as the $^3\Sigma_u^+$ and $A^1\Sigma_u^+$ states, it is essential to treat them within a quasi-degenerate framework. This approach takes into account the small mixing of the two states due to the perturbation. For this purpose, we build up the cumulative second-order Hamiltonian, $\mathbf{H}^{[2]}$, which includes contributions from both the direct couplings and the second-order perturbative corrections,

$$\mathbf{H}^{[2]} \mathbf{c}_i^{[2]} = E_i^{[2]} \mathbf{c}_i^{[2]}. \tag{S5}$$

The matrix element of the cumulative second-order Hamiltonian, $\mathbf{H}^{[2]}$, is given by [68]:

$$H_{X,Y}^{[2]} = \left\langle X \left| \hat{H}^{(0)} + \alpha^2 \hat{H}_{sd}^{(2)} + \alpha^4 \hat{H}_{sd}^{(2)} \frac{\hat{Q}}{E_Y^{(0)} - \hat{H}^{(0)}} \hat{H}_{sd}^{(2)} \right| Y \right\rangle, \tag{S6}$$

where the states X and Y are the states considered within the model space. The operator \hat{Q} is the projector to orthogonal complement to the coupled (X, Y) subspace, *e.g.*, $\hat{Q} = 1 - |X\rangle\langle X| - |Y\rangle\langle Y|$.

For the specific example of the $^3\Sigma_u^+$ (denoted for short by \mathbf{a}_{M_S} , $M_S = 0, \pm 1$) and $A^1\Sigma_u^+$, the triplet states $a_{\pm 1}$ do not couple to any other states at the second-order level, so we only need to consider the diagonal elements for these states. The second-order energy correction for these triplet states is then expressed as,

$$E_{\mathbf{a}_{\pm 1}}^{[2]} = H_{\mathbf{a}_{\pm 1}, \mathbf{a}_{\pm 1}}^{[2]} = \left\langle \mathbf{a}_{\pm 1} \left| \hat{H}^{(0)} + \alpha^2 \hat{H}_{sd}^{(2)} + \alpha^4 \hat{H}_{sd}^{(2)} \frac{\hat{Q}}{E_{\mathbf{a}}^{(0)} - \hat{H}^{(0)}} \hat{H}_{sd}^{(2)} \right| \mathbf{a}_{\pm 1} \right\rangle. \tag{S7}$$

For A and \mathbf{a}_0 there is a coupling at second order, so the matrix elements of the second-order Hamiltonian are

$$H_{\mathbf{a}_0, \mathbf{a}_0}^{[2]} = \left\langle \mathbf{a}_0 \left| \hat{H}^{(0)} + \alpha^2 \hat{H}_{sd}^{(2)} + \alpha^4 \hat{H}_{sd}^{(2)} \frac{\hat{Q}}{E_{\mathbf{a}}^{(0)} - \hat{H}^{(0)}} \hat{H}_{sd}^{(2)} \right| \mathbf{a}_0 \right\rangle, \tag{S8}$$

$$H_{A,A}^{[2]} = \left\langle A \left| \hat{H}^{(0)} + \alpha^2 \hat{H}_{sd}^{(2)} + \alpha^4 \hat{H}_{sd}^{(2)} \frac{\hat{Q}}{E_A^{(0)} - \hat{H}^{(0)}} \hat{H}_{sd}^{(2)} \right| A \right\rangle, \tag{S9}$$

$$H_{a_0, A}^{[2]} = \alpha^4 \left\langle a_0 \left| \hat{H}_{sd}^{(2)} \frac{\hat{Q}}{E_A^{(0)} - \hat{H}^{(0)}} \hat{H}_{sd}^{(2)} \right| A \right\rangle , \quad (\text{S10})$$

$$H_{A, a_0}^{[2]} = \alpha^4 \left\langle A \left| \hat{H}_{sd}^{(2)} \frac{\hat{Q}}{E_a^{(0)} - \hat{H}^{(0)}} \hat{H}_{sd}^{(2)} \right| a_0 \right\rangle . \quad (\text{S11})$$

The two-by-two matrix can be diagonalized, leading to the eigenvalues,

$$E_{a_0}^{[2]} = \frac{H_{a_0, a_0}^{[2]}}{2} (1 + \sqrt{1 + D}) + \frac{H_{A, A}^{[2]}}{2} (1 - \sqrt{1 + D}) , \quad (\text{S12})$$

$$E_A^{[2]} = \frac{H_{A, A}^{[2]}}{2} (1 + \sqrt{1 + D}) + \frac{H_{a_0, a_0}^{[2]}}{2} (1 - \sqrt{1 + D}) , \quad (\text{S13})$$

$$D = 4 \frac{H_{a_0, A}^{[2]} H_{A, a_0}^{[2]}}{(H_{a_0, a_0}^{[2]} - H_{A, A}^{[2]})^2} . \quad (\text{S14})$$

Based on this formalism, we computed a numerical estimate for the second-order coupling of a $^3\Sigma_u^+$ and A $^1\Sigma_u^+$ through the f $^3\Pi_u$ and F $^1\Pi_u$ states, identified as the most important ‘interaction transmission’ partners based on Ref. [69]. Pilot computations suggest that the resulting second-order contribution is on the $10^{-12} E_h$ range, so completely negligible in this work.